



Injection-locked range and linewidth measurements at different seed-laser linewidths using a Fabry–Pérot laser-diode

Jakup Ratkoceri^{1,2} · Bostjan Batagelj¹

Received: 7 April 2018 / Accepted: 21 October 2018 / Published online: 25 October 2018
© Springer Science+Business Media, LLC, part of Springer Nature 2018

Abstract

In this paper we experimentally examine the dependence of the injection-locked range magnitude of a Fabry–Pérot (FP) laser on the linewidth of a seed laser. We measure the enhancement of the incident-power-dependent injection-locked range when changing the seed-light linewidth in three different ranges, starting with tens of GHz, then hundreds of MHz, and up to a few hundred kHz. We notice the progressive shrinkage of the locking range with an increase in the linewidth of the seed source. Simultaneously, the linewidth of a FP laser was measured and the cancellation of multiple longitudinal operating modes as well as a great reduction of linewidth are observed with a self-homodyne measurement.

Keywords Fabry–Pérot laser diode · Semiconductor laser · Injection locking · Locking range · Linewidth reduction

1 Introduction

The Fabry–Pérot (FP) semiconductor laser diode (Kobayashi et al. 1982) offers several advantages that have led to its extensive use as an optical device in photonic applications (Lau et al. 2009). Its small size, efficiency, the absence of maintenance and low cost are just a few of the benefits that semiconductor laser diodes in the form of a Fabry–Pérot resonator cavity offer to modern photonic applications. In addition to these advantages, they require a low-power current source, can be directly modulated up to a few gigahertz and have an operating wavelength from the near ultraviolet to the far infrared (Tartarini et al. 2006). The disadvantage of the FP laser is its relatively wide spectral width (in the range of a few tens of nanometers) due to its multiple longitudinal modes. This is because the FP optical cavity supports multiple frequencies (Ratkoceri and Batagelj 2017). Added to this weakness, the optical output power and the wavelength of the longitudinal modes as well

✉ Jakup Ratkoceri
Jakup.Ratkoceri@fe.uni-lj.si

¹ Radiation and Optics Laboratory, Faculty of Electrical Engineering, University of Ljubljana, Ljubljana, Slovenia

² IPKO Telecommunication, Pristina, Republic of Kosovo

as the number of longitudinal modes in the FP laser are very unstable, and can change due to fluctuations in the current or the temperature of the environment (Šprem et al. 2015).

The injection-locking technique (Lang 1982; Hadley 1986) enables the inexpensive, simple FP laser to operate in an improved single-longitudinal mode regime—a wavelength characteristic that is common in more complex and consequently more expensive laser solutions, built with some form of internal (Ghafouri-Shiraz and Chu 1991; Jabbariet al. 2013) or external (Hisham et al. 2014; Guignard and Besnard 2006) optical feedback. It has been shown that the injection-locked FP laser has great potential for future applications in fiber optics in telecommunication systems (Batagelj et al. 2014) and for extending the performance of today's gigabit-capable passive optical networks (GPONs) (Zhang et al. 2016; Lee et al. 2010). The injection-locked FP laser can be used for colorless optical network units in a wavelength division multiplexing (WDM) passive optical network (PON) (Mun et al. 2008; Xu et al. 2007; Chen et al. 2013) or to support complex optical modulation schemes for high-speed, all-optical data transmission where a narrow linewidth of the laser source is required (Attygalle et al. 2001).

In optical fiber transmission lines, chromatic dispersion is one of the major impairments that affect the transmission quality of the signal (Dar and Jha 2017). Chromatic Dispersion dependency to the linewidth of the laser source (Dar and Jha 2017) makes the injection locking an important factor in enhancing the transmission capabilities of the FP laser source and reducing the influence of the chromatic dispersion (Ratkoceri and Batagelj 2017). On the other hand, it is clear that electronic signal processing imposes a bottleneck for electro-optical systems. Consequently, photonic components are increasingly seen as a means to overcome this bottleneck. The benefit of injection locking is expected in various applications, such as all-optical flip-flops, memory elements and an optical switch that offers a solution for all-optical routing (Zlitni et al. 2012; Jin and Chuang 2006).

The dependency of the locking range on the linewidth of a seed laser, known also as spectral coherence, has, to the best of our knowledge, not yet been examined in detail. For this reason we made measurements of the relationships between the seed laser's linewidth and the FP laser's locking range. The FP laser's linewidth reduction by injection locking is experimentally proven in this paper. We report on the experimental results of the injection-locking phenomenon and we plot the injection range for the side-locked longitudinal mode of the FP laser, based on the results obtained from the experiment.

The paper is organized as follows. In the second section we describe the background of the injection-locking phenomenon. In the third section we experimentally measure, using a self-homodyne measurement technique, the linewidths (spectral coherence) of three seed sources that are later used for the injection locking. In the fourth section we present the injection-locking measurements for three specified linewidths of the seed lasers, i.e., 300 kHz, 100 MHz and 60 GHz. In the fifth section we observe the behavior of the FP laser linewidth in the injection-locked state with respect to the difference in the linewidth of the seed laser's source. Finally, the measurement results are commented on and the conclusions are drawn.

2 Background to injection-locking

The physical phenomenon of locking was first reported by Christiaan Huygens (Lau et al. 2009), when he noticed the synchronization of two pendulum clocks that were hanging on a wall next to each other. Huygens defined this phenomenon as an “odd kind of sympathy” between two pendulum clocks (Zlitni et al. 2012; Krstić et al. 2013; Razavi 2004).

Injection locking is a nonlinear phenomenon of synchronization that occurs when coupling two or more self-sustained oscillators. In the general definition, the synchronization depends on two parameters: the coupling strength between the two systems and the frequency detuning between the frequencies of the oscillators engaged in the synchronization (Krstić et al. 2013).

In an injection-locked laser system, when two lasers are engaged, light from the so-called master laser is seeded into the cavity of the other laser, known as the slave laser, which is oscillating above the threshold. If the optical frequency of the injected light is close enough to one of the cavity modes of the slave laser and it has enough optical power, the injection-locked state of the slave laser can be achieved (Zlitni et al. 2012; Krstić et al. 2013).

The possibility of using an injection-locked semiconductor laser in wavelength-division-multiplexing passive optical networks, where injection-locked lasers can act as a substitute for more expensive, single-mode lasers, offers a very attractive and cost-effective solution (Erzen et al. 2015; Xiong et al. 2012). The possibility of the side-mode injection locking of a FP laser is considered to be an advantage in WDM channel selection over a single-mode, distributed-feed-back (DFB) laser (Jin and Chuang 2005).

Injection locking provides the prospect of improving the fundamental limits of a directly modulated FP laser (Lau et al. 2009). When using a master laser with a low relative intensity noise (RIN), the injection-locked slave laser will exhibit the same RIN transferred from the master laser (Nguyen et al. 2010). The same phenomenon applies to the laser's linewidth, where a reduced linewidth is achieved (Lawrence 2000). The injection-locked laser reduces the frequency chirping (Zlitni et al. 2012) and eliminates the mode-partition noise (Jin and Chuang 2006) in a directly modulated laser. Also, the modulation bandwidth of the injected bandwidth can be improved significantly (Lau et al. 2008; Ali and Abdul-Wahid 2012; Zhou et al. 2008).

The dynamic of the slave laser in the injection-locked state is defined by the rate equation, which is a theoretical foundation for injection-locking analysis. This paper describes the experimental analysis of injection locking, but a detailed model of the FP laser for inter-modal injection locking is expressed by a multi-mode rate equation (Jin and Chuang 2006; Krstić et al. 2013; Lau, Wong, and Wu 2009; Zlitni et al. 2012) with extra terms describing the locking phenomenon.

The injection locking is forced by two mechanisms. The first mechanism occurs with the presence of an external electrical field, when the slave laser's field will change during the time of the injection due to field coupling. The presence of the out-of-phase component will introduce the phase shift and consequently the frequency shift of the slave field, which is given by $\Delta\phi_{SL} = -(c/2n_cL)\sqrt{S_{inj}/S}\sin(\phi_{SL})\Delta\tau$. The second mechanism occurs by changing the gain of the injected field required to maintain the steady state of the slave laser. This will force a shift in the cavity-resonance frequency. This cavity frequency shift is related to the dependence of the refractive index on the gain change, characterized by the linewidth-enhancement factor α . This change in the cavity can be expressed using $\Delta\omega = -(c/2n_cL)\alpha\sqrt{S_{inj}/S}\cos(\phi_{SL})$ (Jin and Chuang 2006; Krstić et al. 2013).

The combination of the two mechanisms, mentioned above, produces the total angular frequency (Lau et al. 2009; Jin and Chuang 2006):

$$\Delta\omega = \omega_i - \omega_0 = -\frac{c}{2n_c L} \sqrt{\frac{S_{inj}}{S} (1 + \alpha^2)} \sin(\phi_{SL} + \arctan\alpha) \quad (1)$$

Equation (1) expresses the locking bandwidth, which is determined by the injection rate and the phase difference.

The semiconductor laser's locking range is set by the angular-frequency detuning ($\Delta\omega = \omega_i - \omega_0$), where ω_i is the master laser's frequency and ω_0 is the cavity-resonance frequency of the slave laser and the injection power ratio r (the ratio of the photon density S_{inj} injected into the slave laser and the photon density S of the injection-locked mode of the slave laser) for which the slave laser is stably locked to the master laser (Jin and Chuang 2006).

The asymmetric locking bandwidth can be obtained for the rate equation (Jin and Chuang 2006; Krstić et al. 2013; Murakami et al. 2003).

$$\Delta\omega_{min} = -\frac{c}{2n_c L} \sqrt{\frac{S_{inj}}{S} (1 + \alpha^2)} < \Delta\omega < \frac{c}{2n_c L} \sqrt{\frac{S_{inj}}{S}} = \Delta\omega_{max} \quad (2)$$

where n_c is the refractive index, L is the laser-cavity length, c is the speed of light and α is the linewidth-enhancement factor. In the theoretical case, from Eq. (2), we see that the symmetrical locking range would be achieved for $\alpha = 0$.

Outside the locking region we have Four Wave Mixing (FWM), which occurs due to the nonlinear interaction between the slave's laser beam and the injected beam of the test laser, where an additional two new frequencies arise, creating four frequencies separated by the same distance between them (Krstić et al. 2013).

The injection-locked laser offers many benefits in terms of the performance of the laser, starting with the linewidth reduction, the reduction of the mode-partition noise, the synchronization, the frequency stabilization, and the modulation suppression (Lawrence 2000; Lau et al. 2009).

3 Linewidth measurements of the seed laser

When the spectral coherence or the linewidth of the laser is addressed the full width at half maximum (FWHM) of its optical spectrum is inspected (Ali and Abdul-Wahid 2012). In our experimental configuration an HP 8153A tunable laser source (TLS) is employed as the seed laser. The wavelength of the seed laser was set to the subsequently needed incident-light wavelength of 1547.660 nm. For the examination of the injection-locked range magnitude's dependency on the linewidth of the seed laser we need to accurately measure and monitor the linewidth of the seed laser.

The seed-laser linewidth measurement is made with a de-correlation of the optical laser spectrum. We use a time delay for the required de-correlation to make a long delay in the self-homodyne detection (Zhou, Chong, and Guo 2008), as presented in schematic in Fig. 1. The 20-km-long single optical fiber G-652D introduced in one arm of the Mach-Zehnder interferometer adds a time delay of approximately 100 μ s. Such an

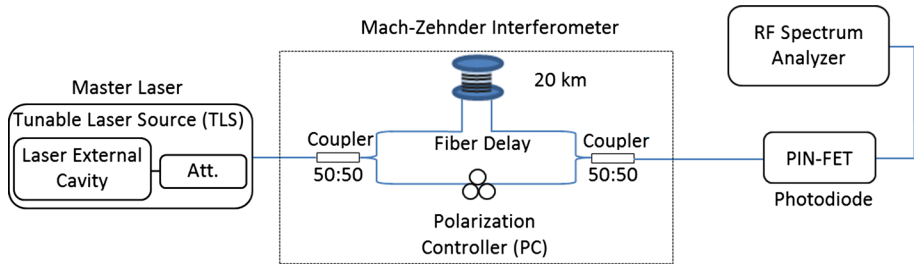


Fig. 1 Self-homodyne detection set-up for seed-laser linewidth measurement

additional time delay makes it possible to measure the laser linewidth down to 10 kHz, which enables us to conduct the required measurements of the seed laser.

A PIN-FET optically integrated receiver is used at the interferometer’s output and the detected result feeds a radio-frequency (RF) spectrum analyzer. In order to eliminate the thermal noise of the photo-receiver and the measuring system, the first step was to measure the noise floor of the linewidth measurement set-up using the RF spectrum when the light of the seed laser was not present.

We had three seed optical sources available, which enabled us to observe the dependency of the injection-locking region with respect to the linewidth of the seed laser. The output power of the TLS was set to 6 dBm during the linewidth measurements. Figure 2 shows the results from the experiment.

It is clear from the graphs in Fig. 2 that we have three optical sources with different linewidths, starting in the regions of kHz, MHz and GHz. To be more precise, we have one optical source with a 300-kHz linewidth, another optical source with 100-MHz linewidth

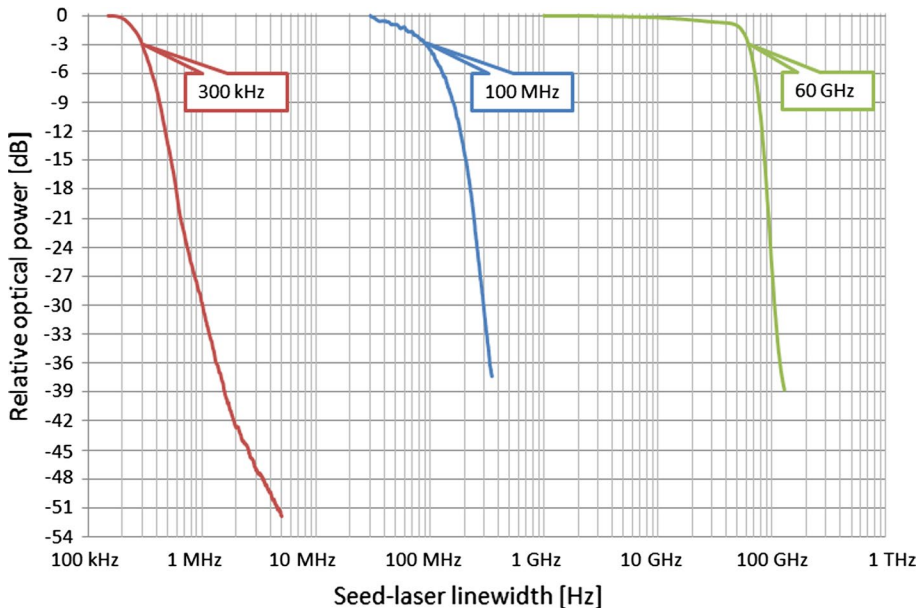


Fig. 2 Measured linewidth of the seed optical source in three spectral coherence conditions

and the broadest source is of 60-GHz linewidth. These differences in the linewidths of the optical sources will enable us to examine the relationship between the linewidth of the seed laser and the locking region of the slave laser.

4 Injection-locking measurements

In this section we analyzed the conditions in which the FP laser is put in the locking state. The 240- μm -long InGaAsP (indium gallium arsenide phosphide) semiconductor FP laser used for this experiment has a threshold current of 10 mA. It is a 1550-nm multiple longitudinal modes laser with the central mode being at 1546.292 nm when measured at 20 °C. Its optimal optical output power is 2 mW (3 dBm).

Our objective is to experimentally investigate the correlation between the injection-locking map of the FP laser and the linewidth of the seed laser. As we mentioned in the previous section, we have available three optical sources with different linewidths and by measuring the injected power S_{inj} from these seed sources and the frequency detuning $\Delta\omega$ we will be capable of plotting and comparing the locking maps of the FP laser in the injection-locking state for the seed-laser sources available.

In accordance with the theory of the injection-locking phenomenon we set-up the experiment to enable seed-laser tuning and slave-laser stabilization, as shown in Fig. 3. We had a reflection style set-up (Lau et al. 2009) for the injection-locking investigation. The tunable laser source is a model HP 8153A with a 6-dBm maximum output power. A polarization controller (PC) was needed in the set-up to verify the polarization dependency of the experimental set-up and to maintain the maximum output power. The temperature controller is very important in order to achieve the operational stability of the FP laser. An optical circulator (OC) enables the injection of the light from the master laser into the cavity of the FP laser and at the same time prevents the light from going back to the master laser. The asymmetric 20/80 optical divider is used to divide the output light from the TLS. Some 20% of the light is sent to the optical spectrum analyzer (OSA1) to control the output power of the TLS, while 80% of the light goes into the optical circulator for injection-locking purposes. With the help of the optical circulator

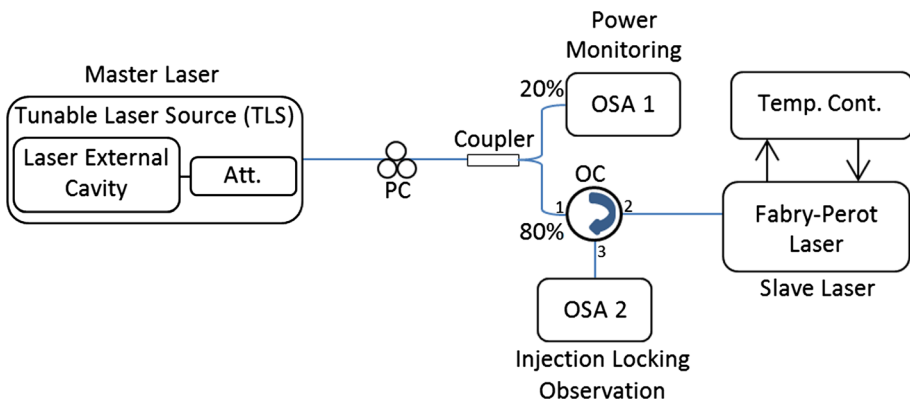


Fig. 3 Schematic of the set-up for the IL measurement

the light from the injection-locked FP laser is guided into the analyzing section. To analyze the injection-locking behavior a second optical spectrum analyzer (OSA2) is used.

For this work we chose inter-modal injection, with the chosen wavelength of the FP laser being the first side-mode on the right of the central longitudinal mode. At 20 °C the chosen wavelength is at 1547.660 nm. The bias current was set to a value of $I = 3I_{th}$. The measured optical spectra of the FP laser in free-running mode and in its injection-locking mode are presented in Fig. 4.

The dotted black line introduces the FP laser's spectrum in free-running mode and, as expected, the FP laser diode in free-running mode has a typical multiple longitudinal modes spectrum with the wavelengths being separated by 1.368 nm. Two side longitudinal modes on the left and on the right of the central longitudinal mode have an approximately 3-dB lower power than the central mode when the FP laser is in the free-running mode. When the FP laser is in injection-locked mode, as shown in Fig. 4 with a solid black line, the injected mode experiences a power increase unlike the other modes that are greatly suppressed, basically offering a single longitudinal mode operational laser. Similar to other literature, also in our experiment we decided to consider that the laser is in the injection-locking mode when the side-mode suppression ratio (SMSR) is higher than 30 dB, and thus the operation of the FP laser is considered to be a single longitudinal mode.

Since in this work one of the tasks is to emphasize the linkage between the linewidth of the seed laser and the locking range of the FP laser, we have inspected the locking maps of the FP laser in the injection-locking state for three different linewidths of the seed optical source, in the kHz, MHz and GHz ranges, and we have also compared the differences in the locking width for these seed lasers.

We analyzed the variations of the FP laser output when the frequency detuning is in highest positive values before switching from injection locking to FWM. Then we analyzed the case when the frequency detuning has the highest negative values before jumping to the FWM state (in the border between injection locking and FWM). This observation is conducted for different injected power values from the seed laser, starting with highest possible input power that the equipment allows and finishing with the input power values, below which it was not possible to lock the FP laser. The results are

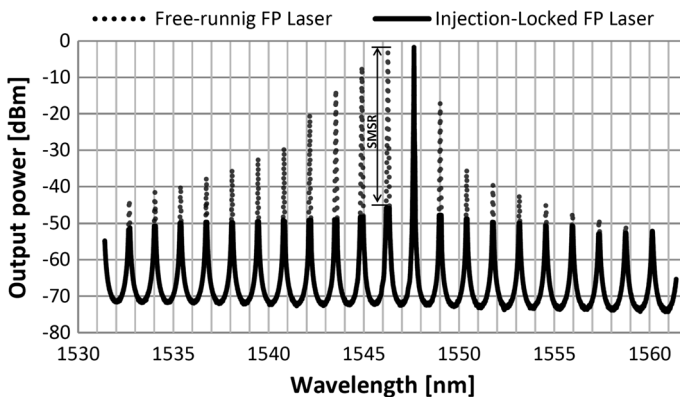


Fig. 4 Optical spectra of FP laser in its free-running mode (dotted black line) and in its injection-locked mode (solid black line)

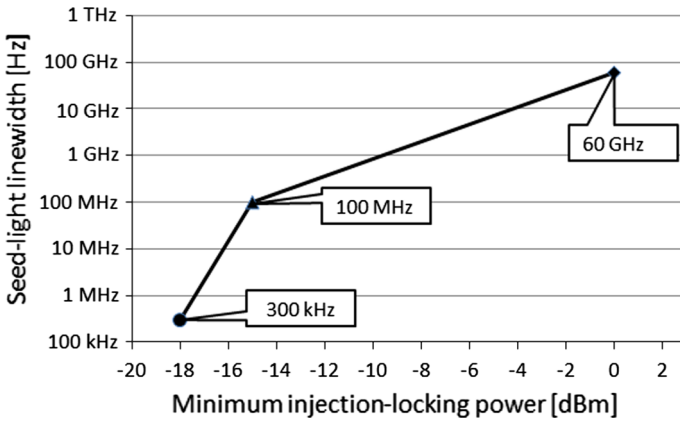


Fig. 5 Minimum injection-locking optical power for the seed optical sources

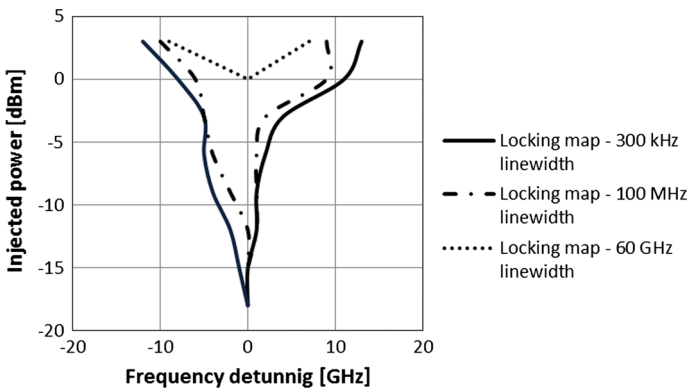


Fig. 6 Injection-locking map of injection-locked FP laser for three linewidths of the seed optical source

presented in Figs. 5 and 6. Three different seed optical sources were considered in these experiments with 300-kHz, 100-MHz and 60-GHz linewidths.

From our experimental results in Figs. 5 and 6 it is clear that we have different injection-locked static locking maps and the locking regimes start from different injected powers of the injection-locked FP laser for different linewidths of the master laser. From the results we see that for a narrower linewidth source the injection locking of a particular longitudinal mode can be achieved with a lower power. From Fig. 5 we see that for the 300-kHz master source the locking state starts from -18 dBm. For the 100-MHz master source the locking of the FP laser starts from -15 dBm. For the broadest master source used in this study as a master source, which is 60 GHz wide, we noticed that we needed a much higher injected power to achieve the injection locking of the FP laser. More precisely, we achieved the injection locking when we increased the injection power to 0 dBm. The locking maps for the three sources are presented in Fig. 6. For the highest input power (3 dBm) applied in this experiment from the seed light at the FP laser’s entrance, the frequency-detuning value at which the FP laser is in the injection-locked state is set to a difference of 7 GHz between

the locking widths generated by the 300-kHz-width source and the 100-MHz-width source, and we have a difference of 10 GHz between the 100-kHz and 60-GHz sources, as shown in Fig. 6. The frequency difference between the two border points on the left- and right-hand sides of the injected mode, when the FP laser enters the injection-locked state, for the 3-dBm injected power from the 300-kHz-width source linewidth is 25 GHz, for 100-MHz-width source it is 18 GHz and for 60-GHz-width source it is 15 GHz only. When the power is decreased to 0 dBm at the input of the FP laser we again have a difference in the injection-locking ranges. For the 300-kHz-width source the frequency difference is 19 GHz and for 100-MHz-width source the frequency difference is 15 GHz. As for the 60-GHz master source, 0-dBm is the lowest point at which we achieved the injecting locking of the FP laser, with an SMSR greater than 30 dB. For the other measured injected powers the difference in the locking range between the 300-kHz and 100-MHz sources decreases with a decrease of the injected power, but it never reaches the same value for both seed sources.

Moreover, our results show that we have a narrower locking map for the case when we use an optical source with a broader linewidth, as presented in Fig. 6, where we have plotted the locking maps of the injection-locked FP laser for three seed lasers. The difference in the locking maps of the FP laser between the optical sources, and which is worth underlining, is when observed for a low input power, where for the 300-kHz-width source it is possible to put the FP laser in the injection-locking state with an input power of -18 dBm, and for the 100-MHz-width source we managed to put the FP laser in the injection-locked mode with the lowest power of -15 dBm. As with the 60-GHz source we needed a higher injected power in the region of 0 dBm.

In general terms, locking bandwidths is a consequence of the injected rate from the master laser and the phase difference between the master- and slave-laser sources and the theoretical background of the achieved locking bandwidth can be summed up from these two mechanisms defined in (1) and (2). However, as in Krstić et al. (2013), the impact of the unlocked modes for the case of multi-longitudinal semiconductor laser in defining the locking range and the stability of the locking map is fundamental for the case of inter-modal injection locking. The general system of the rate equation for the case of the multimode rate equation is enriched with the equation that describes the behavior and the impact of the unlocked modes in the injection-locking process. From Krstić et al. (2013), the locking range defined in (1) and (2) for intermodal injection locking is expanded to:

$$r_{\pm} = \left[\frac{1}{k_c} \left(\pm |\Delta\omega| - \text{sgn}(\Delta\omega) \frac{\alpha}{2} A_m(n_c) \right) \right]^2 \quad (3)$$

where $A_m(n_c)$ is the effective rate of stimulated photon generation for the locked mode m and n_c is the steady-state carrier concentration for the case of the inter-modal injection locking, boundary condition of $\cos(\phi_{SL}) = 0$.

Starting from (1) the locking boundaries between FWM and the locking regime are defined by $\sin(\phi_{SL} + \arctan\alpha) = \pm 1$, which are considered to be the extreme boundaries of the locking range. However, due to the dispersive nature of the semiconductor laser, the presence of the external photons inside the cavity of the slave laser will affect the carrier concentration, which will result in an increase in the active refractive region and, consequently, the gain will be reduced. This increase is proportional to α , which will cause frequency red shifts due to the cavity-resonance decrease. This means that with the same injected ratio r the laser with the higher α will have a broader locking range. From Osinski and Buus (1987), the locking range is increased by $(1 + \alpha^2)^{1/2}$ as found in (2). From Henry

et al. (1982), due to the second mechanism of injection locking explained in Sect. 2, the locking range will be asymmetrical. Alerting the cavity resonance frequency with the presence of the injected field will make the portion of the positive part of the locking range unstable, which causes an asymmetric shrinkage of the positive part of the locking range, which we also noticed in our measurements.

An additional constraint is defined by the fact that $\cos(\theta_m) > 0$, and this will cause a narrower locking range than the boundaries defined by FWM. For the case of the intramodal injection locking the negative value of $A_m(n_c)$, as defined in (3), will add additional shrinkage to the locking boundaries of the positive part of the frequency detuning.

Our results show that the linewidth of the seed-laser source has a direct impact on the injection-locking range of the FP laser. In our case we used three laser sources with kHz, MHz and GHz linewidths. For the narrower linewidth we found that the locking range of the FP laser is broader and for the broader linewidth we have a narrower locking range for the FP laser. These differences in the locking ranges are a consequence of the different linewidths that directly affect the locking ranges. As described by Lau et al. (2009), one of the three main components to determine the magnitude of the directly modulated frequency response is the resonance frequency. From Murakami et al. (2003) we see that with an increase of the frequency detuning we have a resonance-frequency enhancement that is one of the main components in the bandwidth enhancement.

5 Linewidth measurements of the FP laser in the injection-locked mode

When the FP laser is in the injection-locked state, besides the fact that the FP laser is behaving as a single-mode laser, as pointed out earlier in this work, most of the characteristics of the master laser are transferred to the spectrum of the FP laser output. Since the linewidth of the laser is an important feature for the effective operation of the laser, we experimentally analyzed the transformation of the linewidth of the FP laser in the injection-locked mode, for the case when we have 300-kHz-width, 100-MHz-width and 60-GHz-width sources as the master laser. The injection locking was performed as in the previous measurements, at the first right-hand-side mode, from the central longitudinal mode of the FP laser. The FP laser was stabilized at 20 °C. The experimental set-up for the measurement of the FP laser's linewidth characteristics when injection-locked, with a 300-kHz-width source, with a 100-MHz-width source and 60-GHz-width, is shown in Fig. 7. Like in Sect. 3, the Mach–Zehnder interferometer with 20 km of fiber optics is installed in one arm of the interferometer to add a time delay.

The injection-locking part of the experiment provides us with information about the state of the FP laser. As for the linewidth measurement for seed-laser sources, the self-homodyne detection with a long delay is applied to determine the linewidth of the FP laser in the injection-locking state for three optical seed sources.

The first measurement was to find the linewidth of the FP laser in the injection-locking mode when it is pumped with 300-kHz-width light from the TLS. For a better interpretation of the difference between the master-laser linewidth and the FP laser linewidth in the injection-locked state when a seed laser is a 300-kHz-width source, both linewidths are plotted on the same graph (Fig. 8). The dotted line represents the linewidth of the master-source laser and the solid line represents the linewidth of the slave FP laser in the injection-locked mode.

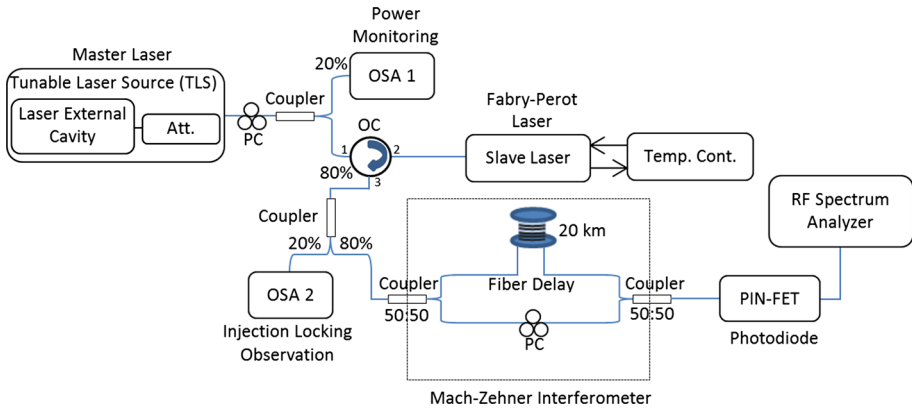


Fig. 7 Experimental set-up for the linewidth measurement of the FP laser in the injection-locked state

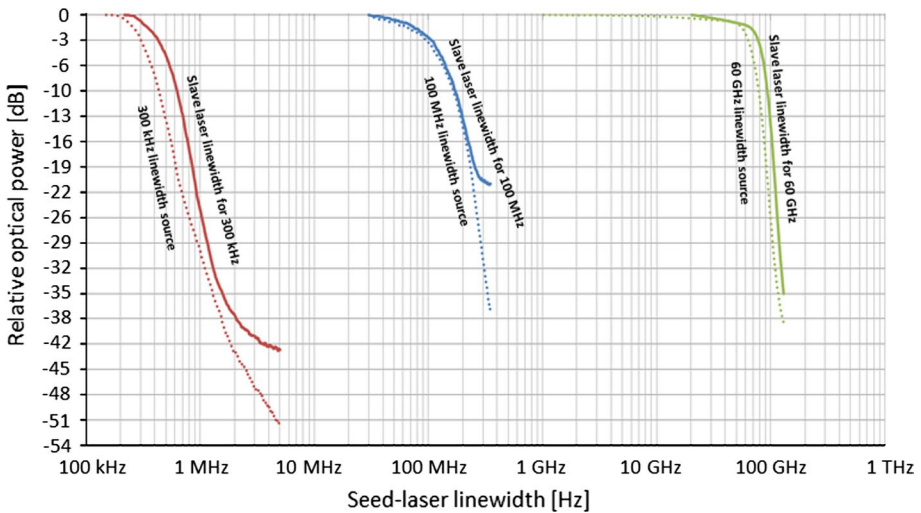


Fig. 8 Linewidth measurement results for the FP laser diode in the injection-locked mode for the three optical seed sources

The experimental result for the linewidth measurement, as presented in Fig. 8, shows that from the peak signal, at 3 dB, for injected-locked FP laser with a 300-kHz-width source, the linewidth that we measured is 125 kHz broader. In the case of the FP laser in the injection-locked mode we noticed that the linewidth at 3 dB from peak signal is approximately 30% larger in comparison to the linewidth of the master laser’s linewidth used for the injection locking.

Also, for the case of the FP laser in the injection-locked state, when the master laser used is 100-MHz-width source, the result can be seen in the same Fig. 8.

From the measured result we found that the linewidth of the FP laser’s spectrum in the injection-locking mode, when the seed light used is 100-MHz-width source, is 11 MHz broader. The linewidth results come from the peak signal at 3 dB. As the result shows, for the case of injection locking when a 100-MHz-width source is used as the master laser, the

linewidth of the FP laser is increased by roughly 10% compared to that of the linewidth of the master laser.

As for the two previous cases, also for the case when we have a GHz linewidth, we notice that a multi-longitudinal FP laser in the injection-locked regime exhibits a similar linewidth behavior transferred from the master laser, with a 15-GHz-broader linewidth, which is an approximately 20% broader linewidth.

For all the measurements we see that the master laser imposes its spectral distribution on the slave laser, with a slightly broader spectral distribution. The FP spectra in the injection-locked mode are similar to the shapes of the seed laser, but with a different linewidth broadening when different seed sources are engaged. We attribute these slight differences in the linewidth broadening to the fact that we do not have a complete transfer of the linewidth due to the limited maximum injected power. From Bondiou (1999), the complete transfer linewidth is achieved when the injected field is strong enough.

6 Conclusion

In this paper we experimentally demonstrated the relationship between the frequency detuning and the injection power in an injection-locking experiment for three optical sources used as seed light. These relationships are shown by an injection-locking graph, where we relied on the frequency selectivity of the master laser and the injected power of the slave laser from the master laser. We showed that with a narrower linewidth of the optical seed source, a broader injection-locked range for the slave laser is obtained. At an incident power of 3 dBm, the locking range is about 30% larger when the linewidth of the seed light is changing from 100 MHz to 300 kHz and there is a 40% larger locking bandwidth if the seed light linewidth is changed from 60 GHz to 300 kHz. This difference in the locking range means that we have higher frequency detuning for a narrower linewidth and with higher frequency detuning we have a resonance-frequency enhancement, which is one of the main components in the bandwidth enhancement.

The performance of the injection-locked FP laser linewidth was also measured. The extensions of the injection-locked FP laser linewidths were presented for all cases of seed-laser sources. These results show that the linewidth of the FP laser in the injection-locked mode approximately replicates the linewidth characteristics of the source laser used as a seed laser for the injection locking, which is a very important feature for the FP laser's applicability, as linewidth-transfer characteristics will enhance the performance of the FP laser.

Acknowledgements The authors acknowledge the financial support of the Slovenian Research Agency (Research Core Funding No. P2-0246 "Algorithms and optimization procedures in telecommunications").

References

- Ali, A.H., Abdul-Wahid, S.N.: Analysis of self-homodyne and delayed self-heterodyne detections for tunable laser source linewidth measurements. *IOSR J. Eng.* **2**(10), 1–6 (2012)
- Attygalle, M., Liu, H., Nirmalathas, A.: An all-optical WDM-to-TDM conversion scheme with simultaneous all-optical synchronization for WDM/OTDM network nodes. *Opt. Quantum Electron.* **33**(7–10), 827–840 (2001). <https://doi.org/10.1023/A:1017556424106>
- Batagelj, B., Janyani, V., Tomazic, S.: Research challenges in optical communications toward 2020 and beyond. *Inf. Midem.* **44**(3), 177–184 (2014)

- Bondiou, M.: Linewidth of an optical injected semiconductor laser. *J. Opt. B Quantum Semiclass. Opt.* **1**, 1–6 (1999)
- Chen, H.Y., Yeh, C.H., Chow, C.W., Sung, J.Y., Liu, Y.L., Chen, J.: Investigation of using injection-locked Fabry–Pérot laser diode with 10% front-facet reflectivity for short-reach to long-reach upstream PON access. *IEEE Photonics J.* **5**(3), 7901208 (2013). <https://doi.org/10.1109/JPHOT.2013.2265219>
- Dar, A.B., Jha, R.K.: Chromatic dispersion compensation techniques and characterization of fiber Bragg grating for dispersion compensation. *Opt. Quantum Electron.* **49**, 108 (2017). <https://doi.org/10.1007/s11082-017-0944-4>
- Erzen, V., Mikulic, M., B. Batagelj.: Frequency-response measurements of an injection-locked Fabry–Pérot laser diode in a colorless WDM-PON. In: 2015 Workshop on Fiber Optics in Access Network FOAN'2015, pp. 26–30 (2015)
- Ghafouri-Shiraz, H., Chu, C.Y.J.: Distributed feedback lasers: an overview. *Fiber Integr. Opt.* **10**(1), 23–47 (1991). <https://doi.org/10.1080/01468039108201603>
- Guignard, C., Besnard, P.: Experimental injection map of semiconductor laser submitted to filtered feedback. *Opt. Quantum Electron.* **38**, 411–428 (2006). <https://doi.org/10.1007/s11082-006-0040-7>
- Hadley, G.: Injection locking of diode lasers. *IEEE J. Quantum Electron.* **22**(3), 419–426 (1986). <https://doi.org/10.1109/JQE.1986.1072979>
- Henry, C.: Theory of the linewidth of semiconductor lasers. *IEEE J. Quantum Electron.* **18**(2), 259–264 (1982). <https://doi.org/10.1109/JQE.1982.1071522>
- Hisham, H.K., Mahdiraji, G.A., Abas, A.F., Mahdi, M.A., Adikan, F.R.M.: Frequency modulation response due to the intensity modulation of fiber-grating Fabry–Pérot lasers. *J. Mod. Opt.* **61**(13), 1081–1091 (2014). <https://doi.org/10.1080/09500340.2014.920536>
- Jabbari, M., Nafar, M., Bahmani-Firouzi, B.: Large signal analysis of distributed feedback laser with three types spatial chirped grating and high reflection: anti reflection facets. *IETE J. Res.* **59**(5), 640–647 (2013). <https://doi.org/10.4103/0377-2063.123771>
- Jin X., Chuang, S.L.: Injection-locking in Fabry–Pérot quantum-well lasers. In: 2005 Semiconductor Device Research Symposium, pp. 438–439 (2005)
- Jin, X., Chuang, S.L.: Bandwidth enhancement of Fabry–Pérot quantum-well lasers by injection-locking. *Solid-State Electron.* **50**(6), 1141–1149 (2006)
- Kobayashi, S., Yamamoto, Y., Ito, M., Kimura, T.: Direct frequency modulation in AlGaAs semiconductor lasers. *IEEE Trans. Microw. Theory Tech.* **30**(4), 428–441 (1982). <https://doi.org/10.1109/tmtt.1982.1131084>
- Krstić, M.M., Crnjanski, J.V., Mašanović, M.L., Johansson, L.A., Coldren, L.A., Gvozdić, D.M.: Multi-valued stability map of an injection-locked semiconductor laser. *IEEE J. Sel. Top. Quantum Electron.* **19**(4), 1501408 (2013). <https://doi.org/10.1109/jstqe.2013.2241026>
- Lang, R.: Injection locking properties of a semiconductor laser. *IEEE J. Quantum Electron.* **18**(6), 976–983 (1982). <https://doi.org/10.1109/JQE.1982.1071632>
- Lau, E.K., Sung, H.K., Wu, M.C.: Frequency response enhancement of optical injection-locked lasers. *IEEE J. Quantum Electron.* **44**(1), 90–99 (2008). <https://doi.org/10.1109/JQE.2007.910450>
- Lau, E.K., Wong, L.J., Wu, M.C.: Enhanced modulation characteristics of optical injection-locked lasers: a tutorial. *IEEE J. Sel. Top. Quantum Electron.* **15**(3), 618–633 (2009). <https://doi.org/10.1109/JSTQE.2009.2014779>
- Lawrence, J. S.: Diode lasers with optical-feedback, optical-injection, and phase-conjugate feedback. Ph.D. Dissertation, Macquarie University (2000)
- Lee, H.K., Cho, H.S., Kim, J.Y., Yoo, S.H., Lee, C.H.: A WDM-PON with an 80 Gb/s capacity based on wavelength-locked Fabry–Pérot laser diode. *Opt. Exp.* **18**(17), 18077–18085 (2010). <https://doi.org/10.1364/OE.18.018077>
- Mun, S.G., Moon, J.H., Lee, H.K., Kim, J.Y., Lee, ChH: A WDM-PON with a 40 Gb/s capacity based on wavelength-locked Fabry–Pérot laser diodes. *Opt. Exp.* **16**(15), 11361–11368 (2008)
- Murakami, A., Kawashima, K., Atsuki, K.: Cavity resonance shift and bandwidth enhancement in semiconductor lasers with strong light injection. *IEEE J. Quantum Electron.* **39**(10), 1196–1204 (2003). <https://doi.org/10.1109/JQE.2003.817583>
- Nguyen, Q.T., et al.: Using optical injection of Fabry–Pérot lasers for high-speed access in optical telecommunications. In: Semiconductor Lasers and Laser Dynamics IV, SPIE Photonics Europe, Proceedings, vol. 7720 (2010). <https://doi.org/10.1117/12.85513>
- Osinski, M., Buus, J.: Linewidth broadening factor in semiconductor laser—an overview. *IEEE J. Quantum Electron.* **23**(1), 9–29 (1987). <https://doi.org/10.1109/JQE.1987.1073204>
- Ratkoceri, J., Batagelj, B.: Comparison of the frequency responses of free-running and injection-locked Fabry–Pérot laser diodes up to 10 GHz. In: 2017 Workshop on Fiber Optics in Access Network FOAN'2017 (2017)

- Razavi, B.: A study of injection locking and pulling in oscillators. *IEEE J. Solid-State Circuits* **39**(9), 1415–1424 (2004). <https://doi.org/10.1109/JSSC.2004.831608>
- Šprem, M., Babić, D., Bosiljevac, M., Šipuš, Z.: Temperature dependence of injection-locked Fabry–Pérot laser emission in WDM-PON architectures. In: 2015 Convention on Information and Communication Technology, Electronics and Microelectronics MIPRO'2015, pp. 74–78 (2015)
- Tartarini, G., Lena, A., Passaro, D., et al.: Harmonic and intermodulation distortion modeling in IM-DD multi-band radio over fiber links exploiting injection locked lasers. *Opt. Quantum Electron.* **38**(9–11), 869–876 (2006). <https://doi.org/10.1007/s11082-006-9055-3>
- Xiong, F., Zhong, W.D., Kim, H.: A broadcast-capable WDM-PON based on polarization-sensitive weak-resonant-cavity Fabry–Pérot laser diodes. *J. Lightw. Technol.* **30**(3), 355–361 (2012). <https://doi.org/10.1109/JLT.2011.2182039>
- Xu, Z., Wen, Y., Zhong, W., Chae, C., Cheng, X., Wang, Y., Lu, C., Shankar, J.: High-speed WDM-PON using CW injection-locked Fabry–Pérot laser diodes. *Opt. Exp.* **15**(6), 2953–2962 (2007)
- Zhang, Z., Zhang, B., Ju, C., et al.: Bidirectional 50 Gb/s/k WDM-PON based on optical intensity modulation and direct detection. *Opt. Quantum Electron.* **48**, 476 (2016). <https://doi.org/10.1007/s11082-016-0751-3>
- Zhou, W., Chong, K.M., Guo, H.: Linewidth measurement of Littrow structure semiconductor laser with improved methods. *Phys. Lett. A* **372**(23), 4327–4332 (2008)
- Zlitni, A.G.R., Krstić, M.M., Gvozdić, D.M.: Modulation response and bandwidth of injection-locked Fabry–Pérot laser diode. *Phys. Scr.* **2012**, 014033 (2012)